An Adaptive Control for a Free-Floating Space Robot by Using Inverted Chain Approach

Satoko Abiko and Gerd Hirzinger
Institute of Robotics and Mechatronics
German Aerospace Center (DLR)
82334, Weßling, Germany
satoko.abiko@dlr.de

***Abstract*— This paper addresses an adaptive control for free-floating space robots in the presence of model uncertainty. Firstly, the operational space dynamics for a free-floating robot is derived with a novel, computationally efficient formulation. Then, by using the new formulation, we propose an adaptive control for a free-floating space robot to compensate the model uncertainty. For performance improvement, a composite adaptive control by combination of the trajectory error and the reaction force is further discussed. To verify the effectiveness of the proposed methods, a three-dimensional realistic numerical simulation is carried out.**

***Index Terms*— Adaptive Control, Inverted Chain Approach, Free-Floating Space Robot, Composite Adaptive Control**

I. Introduction

The necessity of on-orbit servicing robots has been discussed because of the recent international interests in space development and the curiosity to the commercial use on orbit. On-orbit servicing space robots are expected to perform various tasks including capturing a target, constructing a large structure and autonomous maintenance of on-orbit systems.

In the free-floating dynamic scenario, one fundamental task would be the tracking and the positioning of a target grasped by the space robot in operational space. This work addresses the task of following a desired trajectory in operational space while the space robot grasps a target with unknown dynamic properties. This leads to a tracking problem, where a given nominal trajectory has to be tracked, while accounting for the parameter uncertainty.

In ground-based manipulator systems, the dynamic parameter uncertainty affects only dynamic equations. In free-floating space robots, however, the parameter uncertainty appears not only in the dynamic equation but also in kinematics mapping from the joint space to the Cartesian space due to the absence of fixed base. Therefore, the model inaccuracies lead to the deviation of operational space trajectory provided by the kinematic mapping.

One method to deal with this issue can be found in an adaptive control. Xu and Gu proposed an adaptive control scheme for space robots in both joint space and operational space [1], [2]. However, the adaptive control proposed in [1] requires perfect attitude control and the adaptive control in [2] proposes an normal augmentation approach based on an under-actuated system, but demands large computational consuming.

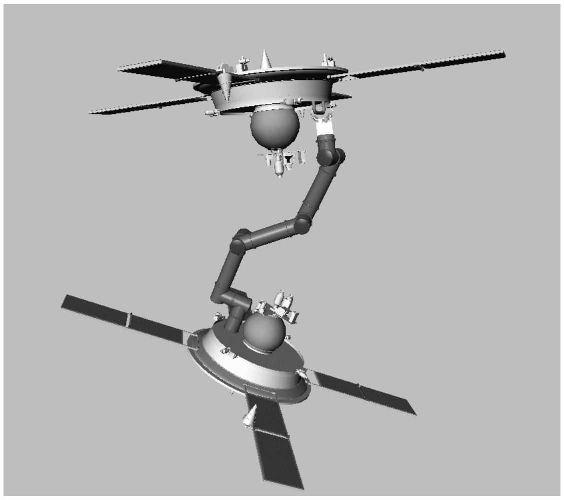

Fig. 1: Chaser-robot and target scenario

In this paper, we propose an adaptive control for a *fully* free-floating space robot in operational space with a novel, computational efficient formulation. This paper particularly focuses on the uncertainty of kinematic mapping. To achieve the desired input torque, it is assumed here that the velocity-based closed-loop servo controller is used as noted in [3].

Since a free-floating space robot does not have any fixed base, we can consider the system switched around and the system can be modeled from the end-effector to the base-satellite. This approach was introduced in [4] and was termed the *inverted chain approach*. The inverted chain approach has a computational advantage compared with the conventional dynamic model for operational space and explicitly explains coupled dynamics between the end-effector and the robot arm. A proposed adaptive control for operational space trajectory tracking is developed based on the inverted chain approach. The control method is verified in simulation for a realistic three-dimensional scenario (See Fig. 1).

The paper is organized as follows. Section II describes the dynamic model of a space robot by the inverted chain approach. Section III discusses the operational space motion control for space robots based on the passivity theorem. Section IV proposes an adaptive control for trajectory tracking in operational space against parameter uncertainties. Section V derives an alternative adaptive control for performance improvement. Section VI illustrates the simulation results with a three-dimensional realistic model. The conclusions are summarized in Section VII.

II. Modeling and equations of motion

This section introduces the model of a space robot. Since the focus of this research is on following a desired trajectory in operational space, it is convenient to refer to operational space schemes.

Due to the lack of a fixed base, one can model a free-floating space robots with two approaches. The general dynamic expressions of free-floating robots use linear and angular velocities of the base and the motion rate of each joint as generalized coordinates [5]. However, by considering the system switched around, modeled from the end-effector to the base, it can be represented by the motion of the end effector and that of the joints in the same structure as in the conventional expression. This scheme is termed the *inverted chain approach* in [4].

The following subsections explain the dynamic equations of the system in the inverted chain approach, for a serial rigid-link manipulator attached to a floating base, as shown in Fig. 2.

A. Equations of motion – Inverted chain approach

Let us consider the linear and angular velocities of the end-effector, $\dot{\boldsymbol{x}}_e = (\boldsymbol{v}_e^T, \boldsymbol{\omega}_e^T)^T \in R^{6\times 1}$, and the motion rate of the joints, $\dot{\boldsymbol{\phi}} \in R^{n\times 1}$ as the generalized coordinates. The equations of motion are expressed in the following form:

$$\begin{bmatrix} \boldsymbol{H}_e & \boldsymbol{H}_{em} \\ \boldsymbol{H}_{em}^T & \boldsymbol{H}_m \end{bmatrix} \begin{bmatrix} \ddot{\boldsymbol{x}}_e \\ \ddot{\boldsymbol{\phi}} \end{bmatrix} + \begin{bmatrix} \boldsymbol{c}_e(\boldsymbol{x}_e, \dot{\boldsymbol{x}}_e, \boldsymbol{\phi}, \dot{\boldsymbol{\phi}}) \\ \boldsymbol{c}_m(\boldsymbol{x}_e, \dot{\boldsymbol{x}}_e, \boldsymbol{\phi}, \dot{\boldsymbol{\phi}}) \end{bmatrix} = \begin{bmatrix} \mathcal{F}_e \\ \boldsymbol{\tau} \end{bmatrix} + \begin{bmatrix} \boldsymbol{J}_e^T \\ \boldsymbol{J}_m^T \end{bmatrix} \mathcal{F}_b. \quad (1)$$

The symbols used here are listed in Table I.

In the case that $\mathcal{F}_b$ is generated actively (*e.g.* jet thrusters or reaction wheels etc.), the system is called a *free-flying* robot. On the other hand, if no active actuators are applied on the base, the system is termed a *free-floating* robot. In this paper, we consider the *free-floating* robot.

B. Equations of motion in operational space

The upper part of (1) clearly describes the equation of motion in operational space:

$$\boldsymbol{H}_e \ddot{x}_e + \boldsymbol{H}_{em}\ddot{\boldsymbol{\phi}} + \boldsymbol{c}_e = \mathcal{F}_e + \boldsymbol{J}_e^T \mathcal{F}_b \quad (2)$$

In a free-floating space robot, only the joint motion can be considered as a generalized coordinate.

$$\begin{aligned} \boldsymbol{H}_e \ddot{x}_e + \boldsymbol{c}_e &= -\boldsymbol{H}_{em}\ddot{\boldsymbol{\phi}} + \mathcal{F}_e + \boldsymbol{J}_e^T \mathcal{F}_b \\ &= \mathcal{F}_i + \mathcal{F}_e + \boldsymbol{J}_e^T \mathcal{F}_b \end{aligned} \quad (3)$$

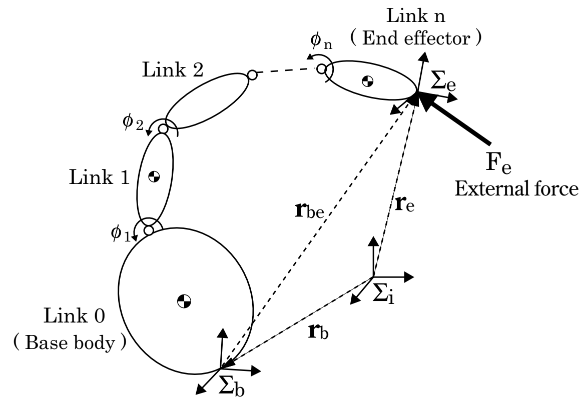

Fig. 2: General model for a space robot

TABLE I: Main notations in dynamic equations

$\boldsymbol{H}_e(\boldsymbol{x}_e, \boldsymbol{\phi})$	$\in R^{6\times 6}$	: inertia matrix of the end-effector.
$\boldsymbol{H}_m(\boldsymbol{x}_e, \boldsymbol{\phi})$	$\in R^{n\times n}$	: inertia matrix of the robot arm.
$\boldsymbol{H}_{em}(\boldsymbol{x}_e, \boldsymbol{\phi})$	$\in R^{6\times n}$	: coupling inertia matrix between the end-effector and the arm.
$\boldsymbol{c}_e$	$\in R^{6\times 1}$	: non-linear velocity dependent term on the end-effector.
$\boldsymbol{c}_m$	$\in R^{n\times 1}$	: non-linear velocity dependent term of the arm.
$\mathcal{F}_e$	$\in R^{6\times 1}$	: force and moment exerted on the end-effector.
$\mathcal{F}_b$	$\in R^{6\times 1}$	: force and moment exerted on the base.
$\boldsymbol{\tau}$	$\in R^{n\times 1}$	: torque on the joints.

where $\mathcal{F}_i = -\boldsymbol{H}_{em}\ddot{\boldsymbol{\phi}}$ stands for a reaction force onto the end-effector due to the robot arm motion.

Remark 1:Input command for the operational space dynamics

The right-hand side in (3) apparently shows the reaction or coupling effect due to the motion of the robot arm with joint acceleration expression. The torque control input does not appear explicitly in (3). Joint acceleration, however, can be achieved by velocity-based closed-loop servo controller straightforwardly as noted in [3]. Therefore, eq. (3) are convenient formulation for constructing a control strategy. Hereafter, $\ddot{\boldsymbol{\phi}}$ is considered as an input command to the system and the appropriate joint acceleration for proper control law is computed. Then, one can refer $\mathcal{F}_i = -\boldsymbol{H}_{em}\ddot{\boldsymbol{\phi}}$ as a reaction force due to the motion of the robot arm, which can be used to analyze the influence of the parameter errors in section IV.

Remark 2:Linearity in the Dynamics Parameters

The linearity of eq. (2) is one of the significant features in the articulated-body system. This characteristic is used for the following derivation of an adaptive control. Eq. (2) can be described by the sum of the equation of motion of each link as follows:

$$\mathcal{F}_e = \frac{d}{dt}\mathcal{L}_e = \boldsymbol{H}_e\ddot{x}_e + \boldsymbol{H}_{em}\ddot{\boldsymbol{\phi}} + \boldsymbol{c}_e, \tag{4}$$

$$\mathcal{L}_e = \sum_{i=0}^{n}\begin{bmatrix} m_i\dot{\boldsymbol{r}}_i \\ \boldsymbol{I}_i\boldsymbol{\omega}_i + \boldsymbol{r}_i \times m_i\dot{\boldsymbol{r}}_i \end{bmatrix}, \tag{5}$$

where $\boldsymbol{I}_i$, $\boldsymbol{\omega}_i$, m_i and $\boldsymbol{r}_i$ stand for the inertia matrix, angular velocity, mass and center of mass for the link i, respectively. Eq. (5), an integral form of the dynamic motion (4), expresses the total linear and angular momentum of the system. Then, once eq. (5) can be linearized with respect to a suitable set of dynamic parameters, the time-derivative of (5), namely eq. (4) can be linear in terms of the dynamic parameters since the dynamic parameters are independent on the motion of the system. Through some calculations, eq. (5) is linearized in terms of a set of the dynamic parameters $\boldsymbol{a}$.

$$\mathcal{L}_e = \boldsymbol{y}(\boldsymbol{x}_e, \dot{\boldsymbol{x}}_e, \boldsymbol{\phi}, \dot{\boldsymbol{\phi}})\boldsymbol{a}. \tag{6}$$

Since the set of the dynamic parameters $\boldsymbol{a}$ is *constant* and is not affected by the motion of the arm, eq. (4) can also be linear with respect to the dynamic parameters, and then eq. (4) can be expressed as a function of a proper set of dynamic parameters $\boldsymbol{a}$.

$$\mathcal{F}_e = \boldsymbol{H}_e\ddot{x}_e + \boldsymbol{H}_{em}\ddot{\boldsymbol{\phi}} + \boldsymbol{c}_e = \boldsymbol{Y}(\boldsymbol{x}_e, \dot{\boldsymbol{x}}_e, \ddot{\boldsymbol{x}}_e, \boldsymbol{\phi}, \dot{\boldsymbol{\phi}}, \ddot{\boldsymbol{\phi}})\boldsymbol{a}, \tag{7}$$

where $\boldsymbol{Y}$ stands for the time-derivative of $\boldsymbol{y}$, which is a function of state values. This insight is significant to derive an adaptive control in Section IV. The choice of the regressor $\boldsymbol{Y}$ and the dynamic parameter vector $\boldsymbol{a}$ is generally arbitrary. In this paper, we assume that only a grasped target includes unknown dynamic parameters, and then the dynamic parameter vector $\boldsymbol{a}$ is defined as an p-dimensional vector containing the mass, center of mass, moment of inertia and product of inertia of the target:

$$\boldsymbol{a} = (m, r_{gx}, r_{gy}, r_{gz}, I_{xx}, I_{yy}, I_{zz}, I_{xy}, I_{yz}, I_{zx},)^T \ (p = 10).$$

III. Trajectory Control in Operational Space

This section shows the trajectory controller in operational space for a free-floating space robot. The control law shown in this section is derived based on the passivity theorem [6].

A. Passivity based trajectory tracking control

Let us define a reference output velocity and a reference output acceleration as follows:

$$\boldsymbol{\eta} = \dot{\boldsymbol{x}}_e^d + \boldsymbol{K}_v\widetilde{\boldsymbol{x}}_e,$$
$$\dot{\boldsymbol{\eta}} = \ddot{\boldsymbol{x}}_e^d + \boldsymbol{K}_v\dot{\widetilde{\boldsymbol{x}}}_e,$$

where $\widetilde{\boldsymbol{x}}_e = \boldsymbol{x}_e - \boldsymbol{x}_e^d$, in which $\boldsymbol{x}_e \in R^{6\times1}$ and $\boldsymbol{x}_e^d \in R^{6\times1}$ depict the output vector and the desired output, respectively. $\boldsymbol{K}_v \in R^{6\times6}$ is a strictly positive definite matrix. The reference error $\boldsymbol{s}$ between the reference output $\boldsymbol{\eta}$ and the actual velocity $\dot{\boldsymbol{x}}_e$ can be described by:

$$\boldsymbol{s} = \boldsymbol{\eta} - \dot{\boldsymbol{x}}_e = \dot{\tilde{x}}_e + \boldsymbol{K}_v\widetilde{\boldsymbol{x}}_e. \tag{8}$$

In the case without any parameter errors, the trajectory tracking control law can be determined by means of the feedback linearization as follows:

$$\ddot{\boldsymbol{\phi}}^u = -\boldsymbol{H}_{em}^+(\boldsymbol{H}_e\dot{\boldsymbol{\eta}} + \boldsymbol{c}_e(\boldsymbol{x}_e, \boldsymbol{\eta}, \boldsymbol{\phi}, \dot{\boldsymbol{\phi}}) + \boldsymbol{\Lambda}\boldsymbol{s}), \tag{9}$$

where $\boldsymbol{\Lambda} \in R^{66}$ denotes a positive definite symmetric constant matrix. $\{\cdot\}^u$ stands for the input command. Note that the control law (9) can be achieved under the condition when $\boldsymbol{H}_{em}$ is nonsingular. Since several researches have already been proposed the treatment of the singularity problem [7]–[9], it is out of focus in this paper.

B. Stability analysis

The stability of the control law (9) can be analyzed by means of the Lyapunov direct method. Here, the following reference error energy is considered as a Lyapunov function:

$$E(t) = \frac{1}{2}\boldsymbol{s}^T\boldsymbol{H}_e\boldsymbol{s}. \tag{10}$$

The time-derivative of E is given as:

$$\begin{aligned}\dot{E}(t) &= \boldsymbol{s}^T(\boldsymbol{H}_e\dot{\boldsymbol{s}} + \frac{1}{2}\dot{\boldsymbol{H}}_e\boldsymbol{s}) \qquad (11)\\ &= \boldsymbol{s}^T(\boldsymbol{H}_e\dot{\boldsymbol{\eta}} - \boldsymbol{H}_e\ddot{\boldsymbol{x}}_e + \frac{1}{2}\dot{\boldsymbol{H}}_e\boldsymbol{s})\\ &= \boldsymbol{s}^T(\boldsymbol{H}_e\dot{\boldsymbol{\eta}} + \boldsymbol{H}_{em}\ddot{\boldsymbol{\phi}} + \boldsymbol{c}_e(\boldsymbol{x}_e, \dot{\boldsymbol{x}}_e, \boldsymbol{\phi}, \dot{\boldsymbol{\phi}}) + \frac{1}{2}\dot{\boldsymbol{H}}_e\boldsymbol{s}),\end{aligned}$$

Since the control command is expressed in eq. (9), $\ddot{\boldsymbol{\phi}} = \ddot{\boldsymbol{\phi}}^u$, (see. *Remark 1* in Sec. II), the derivation of $E(t)$ results in:

$$\dot{E}(t) = -\boldsymbol{s}^T\boldsymbol{\Lambda}\boldsymbol{s} \leq 0, \tag{12}$$

Accordingly, the result of $\dot{E}$ holds always semi-negative and the closed-loop system (2) with (9) is guaranteed to be asymptotically stable. The inequality (12) implies that the steady-state reference error $\boldsymbol{s}$ converges asymptotically to zero, which leads to the steady-state position error also converges to zero.

IV. Adaptive Control

The previous section explained the trajectory control for a free-floating space robot based on the inverted chain approach on the assumption of no dynamic parameter errors. In practical situations, however, the robot arm handles various components whose dynamic properties are not known in advance. Those model inaccuracies may lead to the degradation of the control performance and the deviation of the trajectory tracking from the desired one.

This section proposes an adaptive control for a free-floating space robot against the parameter uncertainties.

A. Influence of the dynamic parameter errors

In the presence of dynamic parameter inaccuracies, the dynamic model in operational space can be described as follows:

$$\widehat{\boldsymbol{H}}_e \ddot{x}_e + \widehat{\boldsymbol{c}}_e = -\widehat{\boldsymbol{H}}_{em}\ddot{\boldsymbol{\phi}} = \widehat{\mathcal{F}}_i, \tag{13}$$

where $\widehat{\{\cdot\}}$ stands for the matrix including dynamic parameter errors. In analogy with (9), the control law derived from the dynamic model (13) becomes:

$$\ddot{\boldsymbol{\phi}}^u = -\widehat{\boldsymbol{H}}^+_{em}(\widehat{\boldsymbol{H}}_e\dot{\boldsymbol{\eta}} + \widehat{\boldsymbol{c}}_e(\boldsymbol{x}_e, \boldsymbol{\eta}, \boldsymbol{\phi}, \dot{\boldsymbol{\phi}}) + \boldsymbol{\Lambda s}). \tag{14}$$

The implementation of the input acceleration (14) to the dynamic system (2), the reaction force due to the motion of the robot arm $\mathcal{F}_i$ and the corresponding expected reaction force $\widehat{\mathcal{F}}_i$ has error $\widetilde{\mathcal{F}}_i$:

$$\begin{aligned}\widetilde{\mathcal{F}}_i &= \mathcal{F}_i - \widehat{\mathcal{F}}_i \\ &= -\boldsymbol{H}_{em}\ddot{\boldsymbol{\phi}}^u + \widehat{\boldsymbol{H}}_{em}\ddot{\boldsymbol{\phi}}^u = -\widetilde{\boldsymbol{H}}_{em}\ddot{\boldsymbol{\phi}}^u,\end{aligned} \tag{15}$$

where $\widetilde{\{\cdot\}}$ stands for the error matrix. With the input acceleration (14), the reaction force $\mathcal{F}_i$ can be described by the corresponding expected force $\widehat{\mathcal{F}}_i$ and the error $\widetilde{\mathcal{F}}_i$ as follows:

$$\begin{aligned}\mathcal{F}_i &= \widehat{\mathcal{F}}_i + \widetilde{\mathcal{F}}_i \\ &= \widehat{\boldsymbol{H}}_e\dot{\boldsymbol{\eta}} + \widehat{\boldsymbol{c}}_e + \boldsymbol{\Lambda s} - \widetilde{\boldsymbol{H}}_{em}\ddot{\boldsymbol{\phi}}^u.\end{aligned} \tag{16}$$

Let us analyze here the stability of the system by means of the Lyapunov function (10). In the closed-loop system (2) with the controller (14), the time-derivative of the Lyapunov function (10) is given by:

$$\begin{aligned}\dot{E}(t) &= \boldsymbol{s}^T(\boldsymbol{H}_e\dot{\boldsymbol{\eta}} + \boldsymbol{H}_{em}\ddot{\boldsymbol{\phi}} + \boldsymbol{c}_e + \frac{1}{2}\dot{\boldsymbol{H}}_e\boldsymbol{s}) \\ &= \boldsymbol{s}^T(\widetilde{\boldsymbol{H}}_e\dot{\boldsymbol{\eta}} + \widetilde{\boldsymbol{c}}_e + \widetilde{\boldsymbol{H}}_{em}\ddot{\boldsymbol{\phi}}^u - \boldsymbol{\Lambda s}).\end{aligned} \tag{17}$$

where *Remark 1* is used, namely $\ddot{\boldsymbol{\phi}} = \ddot{\boldsymbol{\phi}}^u$. As mentioned in *Remark 2*, the dynamic system is able to be linearized with the vector of dynamic parameters $\boldsymbol{a}$ and the regressor $\boldsymbol{Y}$. Then, the above time-derivative can be rewritten by:

$$\dot{E}(t) = \boldsymbol{s}^T(\boldsymbol{Y}\widetilde{\boldsymbol{a}} - \boldsymbol{\Lambda s}), \tag{18}$$

where $\widetilde{\boldsymbol{a}} = \boldsymbol{a} - \widehat{\boldsymbol{a}}$ denotes the parameter estimation error vector. $\boldsymbol{a}$ is an p-dimensional vector containing the unknown dynamic parameters and $\widehat{\boldsymbol{a}}$ is its estimate. The above equality indicates that each component Λ_i in the gain matrix $\boldsymbol{\Lambda}$ needs to meet the following condition in order to obtain the robust system against the model inaccuracies:

$$\Lambda_i \geq \boldsymbol{Y}\widetilde{\boldsymbol{a}} + \mu_i, \;\; (\; i = 1 \cdots p \;) \tag{19}$$

where the constant μ_i is strictly positive. As long as the above condition holds, the controller (14) is robust against the parameter inaccuracies and the tracking error converges to zero.

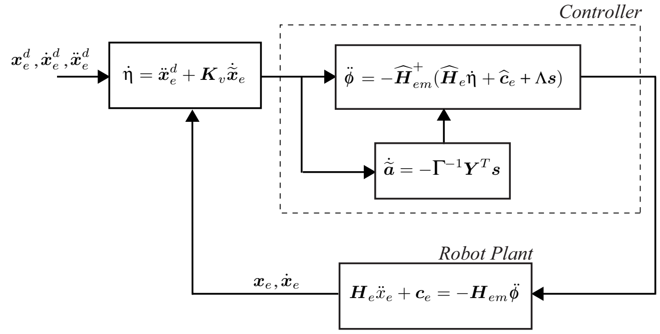

Fig. 3: Control diagram for adaptive trajectory tracking control in operational space

B. Adaptive controller design

Equation (17) suggests two solutions to compensate the parameter uncertainty in the system. One is the improvement of the robustness in the control law (14) with proper design of the gain matrix as shown in (19). The other is to adjust the dynamic parameter itself during the operation, which is called an *adaptive control* [10] [11].

This section proposes an adaptive control in the case without any knowledge of the dynamic parameter in advance, such that the space robot grasps a target whose dynamic parameters is unknown.

Let us consider the following Lyapunov function described with the sum of the reference error energy of the system (10) and the potential energy due to the model uncertainties:

$$V(t) = E(t) + \frac{1}{2}\widetilde{\boldsymbol{a}}^T\boldsymbol{\Gamma}^{-1}\widetilde{\boldsymbol{a}}, \tag{20}$$

where $\boldsymbol{\Gamma} \in R^{p\times p}$ is a positive definite matrix. The time-derivative of (20) becomes:

$$\dot{V}(t) = -\boldsymbol{s}^T\boldsymbol{\Lambda s} + \widetilde{\boldsymbol{a}}^T(\boldsymbol{Y}^T\boldsymbol{s} + \boldsymbol{\Gamma}\dot{\widetilde{\boldsymbol{a}}}). \tag{21}$$

This suggests the following condition should be met to guarantee the system stability,

$$\boldsymbol{Y}^T\boldsymbol{s} + \boldsymbol{\Gamma}\dot{\widetilde{\boldsymbol{a}}} = 0. \tag{22}$$

Then, the following adaptive control law is derived:

$$\dot{\widetilde{\boldsymbol{a}}} = -\boldsymbol{\Gamma}^{-1}\boldsymbol{Y}^T\boldsymbol{s}, \tag{23}$$

where $\widetilde{\boldsymbol{a}} = \boldsymbol{a} - \widehat{\boldsymbol{a}}$ and the parameter vector $\boldsymbol{a}$ is constant.

Consequently, the time-derivative of the Lyapunov function results in:

$$\dot{V}(t) = -\boldsymbol{s}^T\boldsymbol{\Lambda s} \leq 0. \tag{24}$$

The inequality (24) indicates the reference error $\boldsymbol{s}$ converges asymptotically to zero if and only if $\dot{\widetilde{\boldsymbol{x}}}_e \to \boldsymbol{0}$ and $\widetilde{\boldsymbol{x}}_e \to \boldsymbol{0}$. Accordingly, the control law for the trajectory tracking in operational space (14) and the adaptation law (23) yield a stable adaptive controller. Fig. 3 shows the control diagram for the proposed adaptive control.

V. Composite Adaptive Control

The adaptive controller developed in the previous section uses the tracking error to extract the parameter information. To obtain the parameter information, however, one can find various candidates [12]. One possible candidate is the prediction error, which is generally used for parameter estimation. In this section, an alternative adaptive control law is presented, which is developed with the combination of the tracking error and the reaction force as the prediction error. Here the reaction forces due to the motion of the robot-arm is supposed to be measured by the force/torque sensor attached on the end-effector, to which the target is attached. The measurement values are used for parameter adaptation together with the nominal adaptive control law (23).

In analogy with Section II, the reaction forces on the end-effector is able to be linearized with a proper set of the dynamic parameters $\boldsymbol{a}$ as $\mathcal{F}_e^{F/T} = \boldsymbol{W}\boldsymbol{a}$ and its prediction error can be described as $\widetilde{\mathcal{F}}_e^{F/T} = \boldsymbol{W}\widetilde{\boldsymbol{a}}$, where $\boldsymbol{W}$ stands for the regressor. The detail derivation is omitted in this paper.

Then, the adaptive control law (23) is extended to the following expression combined with the tracking error and the predicted reaction force error:

$$\dot{\tilde{\boldsymbol{a}}} = -\boldsymbol{\Gamma}^{-1}\{\boldsymbol{Y}^T\boldsymbol{s} + \boldsymbol{W}^T\boldsymbol{R}\widetilde{\mathcal{F}}_e^{F/T}\} \ , \tag{25}$$

where $\boldsymbol{R} \in R^{6\times6}$ is a uniformly weighting matrix. Eq. (25) can be rewritten as:

$$\dot{\tilde{\boldsymbol{a}}} + \boldsymbol{\Gamma}^{-1}\boldsymbol{W}^T\boldsymbol{R}\boldsymbol{W}\widetilde{\boldsymbol{a}} = -\boldsymbol{\Gamma}\boldsymbol{Y}^T\boldsymbol{s}, \tag{26}$$

which indicates a time-varying low-pass filter and that parameter and tracking error convergence in composite adaptive control can be smoother and faster than the nominal adaptive control only.

To analyze the stability of the system applied the above composite adaptive control law and the trajectory tracking control, the Lyapunov function (20) is considered again. The time-derivative of (20) is derived as (21). Since the adaptive control law is determined by (25), substitution of (25) into (21) leads to the following inequality:

$$\dot{V}(t) = -\boldsymbol{s}^T\boldsymbol{\Lambda}\boldsymbol{s} - \widetilde{\boldsymbol{a}}^T\boldsymbol{W}^T\boldsymbol{R}\boldsymbol{W}\widetilde{\boldsymbol{a}} \le 0, \tag{27}$$

which describes that the reference error $\boldsymbol{s}$ and the prediction error asymptotically converge to zero if the desired trajectories are bounded. If the trajectories are persistently exciting and uniformly continuous, the estimated parameters converge asymptotically to the real ones.

VI. Simulation Study

This section presents the numerical simulation results of a realistic three-dimensional model as shown in Fig. 1. In this simulation, the chaser-robot is assumed to track a given trajectory while it grasps firmly a target including unknown dynamic properties. The initial total linear and angular momentum for whole system are supposed to be zero in the simulation. The chaser robot has a 7 DOF manipulator mounted on the base satellite, whose dynamic parameters are shown in Table II. The robot arm has one redundancy with respect to the end-effector motion, then the null-space can be used for an additional task. In the simulation examples, the target parameters of the planned motion are supposed to be zero, while those of the controlled motion in Table III, giving the extent of uncertainty introduced in the system.

TABLE II: Dynamic parameters for a chaser-robot

	mass $[kg]$	$I_{xx}[kgm^2]$	$I_{yy}[kgm^2]$	$I_{zz}[kgm^2]$
Base	140	18.0	20.0	22.0

	mass $[kg]$	$I\ [kgm^2]$
Each Link	3.3	0.0056

TABLE III: Dynamic parameters for a target

mass $[kg]$	$I_{xx}[kgm^2]$	$I_{yy}[kgm^2]$	$I_{zz}[kgm^2]$
87.5	11.25	12.5	12.5

The adaptation gain $\boldsymbol{\Gamma}$ in eq. (23) is determined by:

$$\boldsymbol{\Gamma} = diag([\ 5\times10^3,\ 10,\ 10,\ 10,\ 5\times10^2,\ 5\times10^2,\ 5\times10^2,\ 5\times10^{-4},\ 5\times10^{-4},\ 5\times10^{-4}\ ]).$$

The control gains $\boldsymbol{\Lambda}$ and $\boldsymbol{K}_v$ in eq. (14) are set to be:

$$\boldsymbol{\Lambda} = diag([\ 20,\ 20,\ 20,\ 3000,\ 3000,\ 3000\ ]),$$
$$\boldsymbol{K}_v = diag([\ 10,\ 10,\ 10,\ 1000,\ 1000,\ 1000\ ]).$$

The weighing matrix $\boldsymbol{R}$ in the composite adaptive control (25) is determined as:

$$\boldsymbol{R} = diag([\ 0.5,\ 0.5,\ 0.5,\ 0.5,\ 0.5,\ 0.5\ ]).$$

Figures 4 and 5 illustrate the desired and actual trajectories in Cartesian space. Fig. 4 shows the case with parameter deviations but without adaptive control. Fig. 5 shows the case with adaptive control (21). The left graphs depict the trajectory in xy plane and the right graphs show the trajectory in xz plane in Cartesian space. In the graphs, the solid line depicts the desired trajectory and the dashed line depicts the actual trajectory, respectively. It is clearly observed that the end effector follows the trajectory when the adaptive control is activated, even though the parameter deviations exist, while in the case without adaptive control law, the end effector deviates the desired trajectory, due to the model errors. Fig. 6 depicts the typical examples for the parameter adaptation process when the adaptive control law is applied. Note here that the adjusted dynamic parameters do not have to converge to the real ones since the demanded task is to follow a given trajectory. If one would like to identify real values, the persistent excitation of the input command is required.

Furthermore, the composite adaptive control (25) is verified in the same condition. The actual trajectory follows the desired one as well as the normal adaptive control (23). However, the tracking error is improved since more information

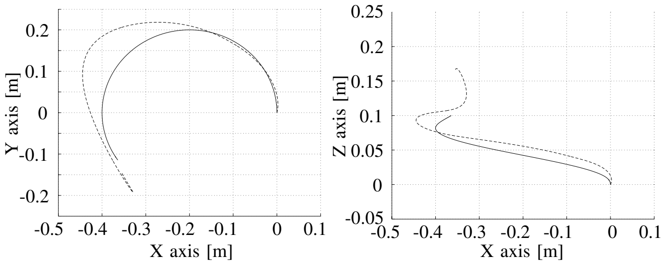

(a) XY Plane (b) XZ Plane

Fig. 4: Trajectory without adaptive control

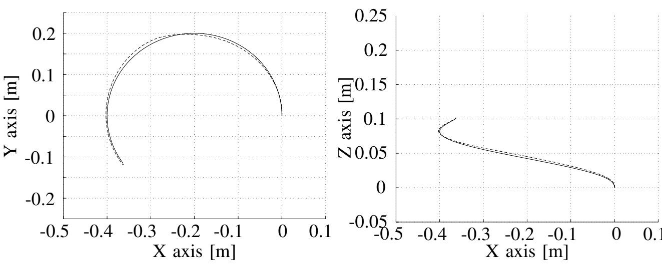

(a) XY Plane (b) XZ Plane

Fig. 5: Trajectory with adaptive control

of the parameters are utilized. Here we evaluate the tracking error with the root mean square error (RMS) in Table IV. In the table, "w/o AC", "with AC" and "with CAC" stand for the case without adaptive control, with adaptive control and the case with composite adaptive control, respectively. The simulations verify that the proposed adaptive controls are effective to achieve the trajectory tracking against the parameter uncertainties with parameter adaptation control.

VII. CONCLUSIONS

In this paper, we proposed an adaptive control for a free-floating space robot by using the inverted chain approach, which is a unique formulation for space robots compared with that for ground-based manipulator systems. This gives the advantage of linearity with respect to the inertial parameters for the operational space formulation and has computational efficiency.

In a free-floating space robot, the dynamic parameters affect not only its dynamics but also its kinematics. By paying attention to the internal dynamics between the end-effector motion and the joint motion, we developed an adaptive control for operational space trajectory tracking in the presence of model uncertainties. To improve the adaptive control performance, a composite adaptive control by using the information of the tracking error and the reaction force is further discussed. The proposed control methods are verified by realistic numerical simulations. The simulation results

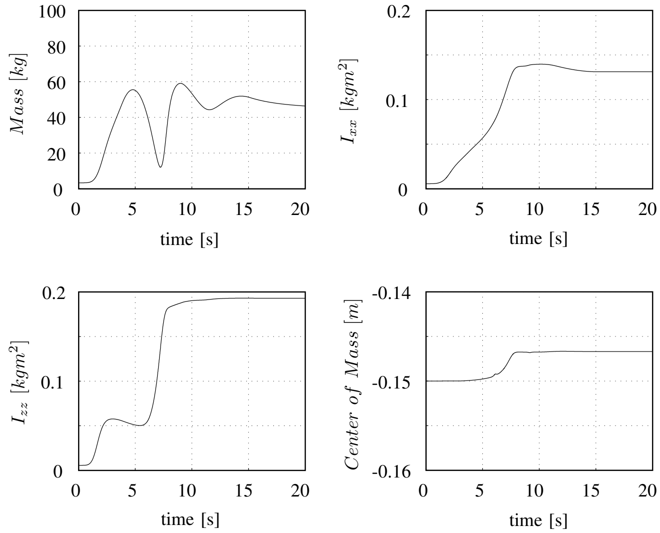

Fig. 6: Adaptation process of the parameters

TABLE IV: Root Mean Square error for tracking error

	w/o AC	with AC	with CAC
RMS error	0.0388	0.0046	0.0032

clearly show that the proposed adaptive controls are effective against the dynamic parameter errors.

REFERENCES

[1] Y. Xu, H.-Y. Shum, J.-J. Lee, and T. Kanade, "Adaptive Control of Space Robot System with an Attitude Controlled Base," in *Proc. of the 1992 Int. Conf. on Robotics and Automation*, Nice, France, May 1992, pp. 2005 – 2011.

[2] Y. L. Gu and Y. Xu, "A Normal Form Augmentation Approach to Adaptive Control of Space Robot Systems," in *Proc. of the 1993 IEEE Int. Conf. on Robotics and Automation*, vol. 2, Atlanta, USA, May 1993, pp. 731 – 737.

[3] A. Konno, M. Uchiyama, Y. Kito, and M. Murakami, "Configuration-Dependent Vibration Controllability of Flexible-Link Manipulators," *Int. Journal Robot. Research*, vol. 16, no. 4, pp. 567 – 576, 1997.

[4] S. Abiko, R. Lampariello, and G. Hirzinger, "Impedance control for a free-floating robot in the grasping of a tumbling target with parameter uncertainty," in *The 2006 IEEE/RSJ Int. Conf. on Intelligent Robots and Systems*, Beijing, China, Oct. 2006, pp. 1020 – 1025.

[5] Y. Xu and T. Kanade, Eds., *Space Robotics: Dynamics and Control*. Kluwer Academic Publishers, 1993.

[6] A. van der Schaft, *L_2-Gain and Passivity Techniques in Nonlinear Control*. Spriger-Verlag, 2000.

[7] D. N. Nenchev, Y. Tsumaki, and M. Uchiyama, "Singularity-Consistent Parameterization of Robot Motion and Control," *Int. Journal of Robotics Research*, vol. 19, no. 2, pp. 159 – 182, Feb. 2000.

[8] Y. Tsumaki, P. Fiorini, G. Chalfant, and H. Seraji, "A Numerical SC Approach for A Teleoperated 7-DOF Manipulator," in *Proc. of the 2001 IEEE Int. Conf. on Robotics and Automation*, Seoul, Korea, May 2001, pp. 1039 – 1044.

[9] V. Senft and G. Hirzinger, "Redundant Motions of Non Redundant Robots - A New Approach to Singularity Treatment," in *Proc. of the 1995 IEEE Int. Conf. on Robotics and Automation*, Nagoya, Japan, May 1995, pp. 1553 – 1558.

[10] J. J. E. Slotine and W. Li, "On the Adaptive Control of Robot Manipulators," *The Int. Journal of Robotics Research*, vol. 6, no. 3, pp. 49 – 59, 1987.

[11] ——, "Adaptive Manipulator Control: A Case Study," *IEEE Transactions on Automatic Control*, vol. 33, no. 11, pp. 995 – 1003, 1988.

[12] J. J. E. Slotine and W. Li, Eds., *Applied Nonlinear Control*. Prentice Hall, 1991.